Available online at www.sciencedirect.com
ScienceDirect
Polymer 48 (2007) 3717–3725
polymer
www.elsevier.com/locate/polymer

Nanostructured thermotropic PBLG–PDMS–PBLG block copolymers

E. Ibarboure, E. Papon, J. Rodríguez-Hernández*

Laboratoire de Chimie des Polymères Organiques, University Bordeaux I; ENSCPB; CNRS; UMR 5629, 16, Pey Berland, F-33607 Pessac, France

Received 6 February 2007; received in revised form 17 March 2007; accepted 10 April 2007
Available online 4 May 2007

Abstract

We report on the nano-organization and the thermal behavior of a series of triblock copolymers composed of a central soft polydimethylsiloxane (PDMS) and two polypeptide (poly-γ-benzyl-L-glutamate) blocks. Peptide blocks with varied lengths and therefore different secondary structures (β-sheet or α-helical) were attached to the PDMS central block. These two blocks are incompatible and microphase separate into different morphologies elucidated by polarized optical microscopy (POM), small-angle light scattering (SALS), X-ray spectroscopy (SAXS, WAXS) and atomic force microscopy (AFM). We demonstrate that the relative ratio of PBLG to PDMS direct both the type of nanodomain morphologies formed and also modifies the transition temperature. Each of these block copolymers have shown a reversible transition associated to its thermotropic liquid crystal behavior. At temperatures above the transition, the self-assembled structures are disrupted and prevented the organization at larger scales.

Keywords: Self-assembly; Rodlike; Isotropization

1. Introduction

Block copolymers are made by covalent attachment of at least two different homopolymers. The blocks, which are usually incompatible in nature, generate self-assembled structures not only in solution but also in bulk, after microphase separation. The order, thereby induced depends on several molecular parameters such as relative block lengths, incompatibility and block interactions (e.g. H-bonding and electrostatic interactions) or temperature [1]. Designing new organized functional materials consequently requires the fine adjustment of all these parameters.

Efforts are currently being focused on the elaboration of organized polymeric materials that display the additional ability to change their function and/or structure, in response to external physical, chemical or electrical stimuli. Such so-called ''intelligent materials'' react to the various impulses by changing back and forth in many ways, including shape, surface energy, permeation rates, reaction rates or molecular recognition [2]. Temperature is one of the most common stimuli in environmentally responsive polymer systems, and temperature-sensitive materials have potential interest for a wide range of applications. One example is the preparation of ''on–off'' membranes [3] that are able to modulate diffusion profiles; in this case, the membrane surface was appropriately functionalized with temperature-responsive polymer chains. Equally, slight temperature variations have been shown to dramatically change both surface and bulk properties of liquid crystalline polymers. Consequently, changes from a rigid and ordered structure to an isotropic phase largely affect parameters such as wettability and, even, adhesive properties [4]. Other temperature-responsive systems have been utilized to manufacture microfluidic devices which can self-control microscale flow as well as separate, purify, analyze or even deliver biomolecules [5].

Liquid crystal polymers, which are expected to produce high degrees of molecular orientation and order, constitute excellent candidates to direct self-assembly. They inherently possess a degree of molecular order: they can exhibit different types of organization, depending either on the concentration

* Corresponding author. Tel.: +33 54000 6574; fax: +33 54000 8487.
E-mail address: jrodriguez@enscpb.fr (J. Rodríguez-Hernández).

0032-3861/$ - see front matter © 2007 Elsevier Ltd. All rights reserved.
doi:10.1016/j.polymer.2007.04.046

when dissolved (lyotropic liquid crystal) or on the temperature when in melt (thermotropic liquid crystal) [6]. There are two main ways to obtain thermotropic liquid crystalline polymers: the incorporation of side-chain liquid crystalline polymers with mesogenic groups attached to a polymer backbone [7] or else main-chain liquid crystalline polymers with mesogenic groups incorporated into a polymer backbone [8]. The thermotropic properties of certain polypeptides, the focus of this study, have previously been reported with liquid crystal behavior being obtained, either by modification of the amino acid structure with alkyl chains [9] or mesogenic groups [10–12], or by copolymerization of long alkyl chain poly(glutamates) [13,14]. Generally, at high temperatures, the introduction of side mesogenic groups alters the polypeptide helical structure, so that self-assembly is prevented and the resulting system is rather disordered.

We consider here a particular triblock copolymer system that combines two rigid rod-like liquid crystal blocks formed by polypeptides, poly(γ-benzylester-L-glutamate) (PBLG), with low T_g, and therefore soft, central polydimethylsiloxane (PDMS) block. In a previous study we demonstrated the ability of these block copolymers to order themselves in multiple length scales (double hexagonal organization) [15]. Although major morphological changes have occurred at long length scales when heated to a certain temperature, at a local level, the hexagonal structure of the polypeptide was conserved at temperatures of as high as 200 °C. In this paper, we study both the melt nano-structures as well as their associated thermal transitions for the same type of triblock copolymers ($PBLG_x$–$PDMS_m$–$PBLG_x$) in which the polypeptide segment length was varied. Although several similar triblock copolymers in which the central block is formed by PB [16,17] or PEO [18] have been already described in the literature the unprecedented thermal properties of the PDMS copolymers have been never reported.

2. Experimental section

2.1. Materials

N,*N*′-dimethylformamide (DMF) and tetrahydrofuran (THF) were distilled from CaH_2 under reduced pressure and stored over molecular sieves under an argon atmosphere. γ-Benzyl-L-glutamate *N*-carboxyanhydride (Bn-Glu NCA) was prepared following previously reported procedures [19] and was recrystallized prior to use from ethyl acetate and hexane. All other solvents were obtained from commercial suppliers and used as received.

2.2. Synthesis

The methodology previously reported by Kumaki et al. [20] for the preparation of similar triblock copolymers has been slightly modified. A dried Schlenk flask was charged with an amount of γ-benzyl-L-glutamate NCA and dissolved in a mixture of DMF/THF 20:80. Then, a commercially available poly(dimethylsiloxane), bis(3-aminopropyl) terminated previously dissolved in the same solvent mixture was added to the solution. Several cycles of vacuum/N_2 were performed to purge the Schlenk and to avoid the presence of humidity in the reaction media. After five days at room temperature, the reaction product was precipitated in water and extensively washed with diethyl ether in order to eliminate rests of decomposed monomer and unreacted initiator.

2.3. Characterization

^{1}H NMR spectra of the copolymers were recorded at room temperature on a Bruker Avance 400 MHz spectrometer using the residual proton resonance of the deuterated solvent as internal standard. Average molar masses and molar mass distributions of the samples were determined by size exclusion chromatography (SEC) using a Varian 9001 pump with both a refractive index (Varian RI-4) and a UV detector (Spectrum Studies UV 150). Calibration was obtained using narrowly distributed polystyrene standards and THF as the mobile phase at a flow rate of 0.5 ml min^{-1}.

Differential scanning calorimetry (DSC) measurements were performed on a DSC Q100 apparatus from TA Instruments. Samples were first heated from −90 °C to 220 °C and consecutively cooled and heated in a second run. All experiments were performed at a rate of 10 °C min^{-1}.

Polarized optical microscopy images have been obtained using a Leitz optical microscope equipped with a camera (SONY) in combination with a Mettler-Toledo FP2 hot stage. Films were prepared by solvent casting from a solution of 20 wt% of the triblock copolymer in THF.

Small-angle light scattering was carried out on the films using a 1 mW He–Ne gas laser source ($\lambda = 632.8$ nm). Linearly polarized laser light was scattered by the sample and then filtered with an analyzer polarized perpendicularly (Hv) to the polarization direction of the incident light. The scattering pattern was imaged on a screen behind the analyzer and recorded with the high resolution CCD camera with a q range from 1.4×10^{-5} Å^{-1} to 3×10^{-3} Å^{-1}.

X-ray diffraction experiments have been performed using a Nanostar (Bruker AXS) device. A ceramic fine-focus X-ray tube has been used in a point focus mode. The tube is powered with a Kristalloflex K760 generator operating at 40 kV, 35 mA. The primary beam is collimated with cross-coupled Göbel mirrors and a pinhole of 0.1 mm id providing a CuK radiation (1.54 Å wavelength). A Hi-Star position-sensitive area detector (Siemens-AXS) was used to record the scattering patterns obtained at two different distances between the sample and detector: 106 and 23 cm. The scattering vector $q = (4\pi/\lambda)\sin(\theta/2)$, where λ is the wavelength and θ the scattering angle.

AFM images were recorded in air with a Nanoscope IIIa microscope operating in tapping mode (TM). The probes were commercially available silicon tips with a spring constant of 42 N m^{-1}, a resonance frequency of 285 kHz, and a typical radius of curvature in the 10–12 nm range. Both the topography and the phase signal images were recorded with a resolution of 512×512 data points. Samples for atomic force

microscopy analysis (AFM) were prepared by solvent casting at room temperature from THF solutions. Typically, 100 μl of a dilute solution (1 wt%) was casted on a silicon wafer substrate.

3. Results and discussion

The series of A–B–A triblock copolymers was obtained using a commercially available α,ω-diaminopropyl dimethylsiloxane (PDMS) as the central B block (Fig. 1). The terminal amine groups were used as initiators for the ring-opening polymerization of α-amino acid *N*-carboxyanhydrides following the primary amine mechanism [21]. The amino acid selected for this study was γ-benzylester-L-glutamate *N*-carboxyanhydride that has the ability both of forming intramolecular H-bonds that lead to stable α-helical structures and exhibit a liquid crystal behavior [6]. The characterization of the polymers employed throughout this contribution was carried out by ^{1}H NMR and GPC and has been described in a previous contribution [15].

Whereas the molar mass of the B block was maintained constant (30 units) and the size of the A blocks was varied from 4 to 40 units by controlling the initiator to monomer ratio introduced in the feed. Variation in the A block length may have two main consequences. First, taking into account only geometrical aspects since the A to B ratio changes, the morphologies obtained may be different [22]. Equally, as it has been previously reported, poly(γ-benzylester-L-glutamate) can be found in different secondary structures, i.e. random coil, β-sheet or α-helical. The preferential formation of one of these structures in bulk is dominated amongst others by the chain length of the polypeptide. Chain lengths below 20 will show a mixture of α-helix and β-sheet with an increase of the latter in shorter chains. Above 20 units, the helical structure dominates [23]. As depicted in Table 1, the systems under study exhibit a continuous variation in the polypeptide conformation from β-sheet to α-helix with increasing chain lengths [15]. The secondary structure in polypeptides can be determined by FTIR spectroscopy thanks to their characteristic amide bands. Polypeptides with longer chain lengths (23 and 40 units) exhibit two bands in this region, the amide I (1650 cm^{-1}) and amide II (1550 cm^{-1}) bands and thus reveal the presence of a α-helical conformation. Shorter polypeptide chain lengths' spectra exhibit in addition a third band at 1630 cm^{-1} indicating the formation, at least partially, of a β-sheet structure.

The phase transition temperatures and their dependence on the triblock copolymers composition were investigated by means of differential scanning calorimetry (DSC) experiments carried out from −130 °C to 200 °C. Below 0 °C, we observed four transitions typically observed for PDMS homopolymer: a glass transition (−127 °C) followed by a cold crystallization (−98 °C) and two melting transitions (−77 °C and −43 °C) [24]. Above zero and during the second heating run (Fig. 2) all block copolymers showed first a glass transition temperature

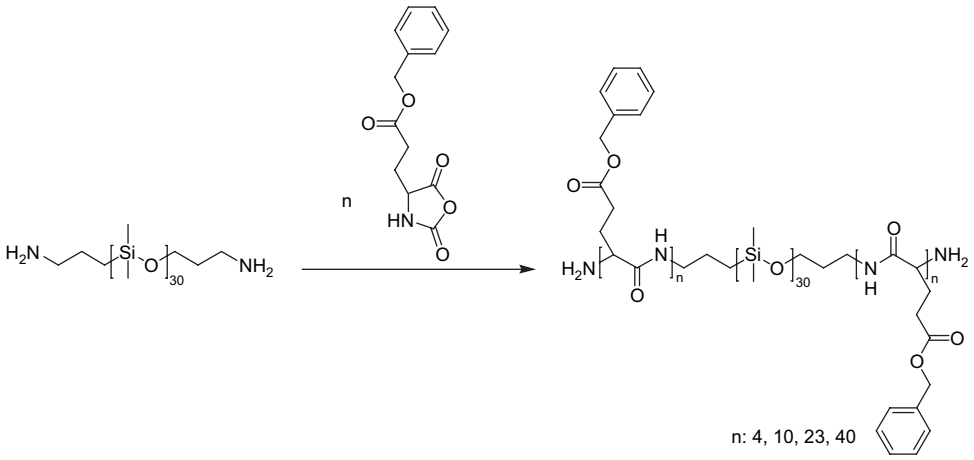

Fig. 1. Synthesis of A–B–A triblock copolymers PBLG–PDMS–PBLG.

Table 1
Molecular characteristics, secondary conformation and thermal transitions of the triblock copolymers PBLG–PDMS–PBLG

Targeted composition	Obtained composition[a]	Polypeptide secondary conformation[b]	Glass transition (°C)[c]	Temperature of the reversible transition (°C)[c]
$PBLG_5$–$PDMS_{30}$–$PBLG_5$ (**1**)	$PBLG_4$–$PDMS_{30}$–$PBLG_4$	Mainly β-sheet	13.0	123.4
$PBLG_{10}$–$PDMS_{30}$–$PBLG_{10}$ (**2**)	$PBLG_{10}$–$PDMS_{30}$–$PBLG_{10}$	β-sheet/α-helix	16.1	152.0
$PBLG_{20}$–$PDMS_{30}$–$PBLG_{20}$ (**3**)	$PBLG_{23}$–$PDMS_{30}$–$PBLG_{23}$	Mainly α-helix	16.8	151.4
$PBLG_{40}$–$PDMS_{30}$–$PBLG_{40}$ (**4**)	$PBLG_{40}$–$PDMS_{30}$–$PBLG_{40}$	α-helix	17.5	77.5

[a] Calculated from ^{1}H NMR spectra.
[b] Determined for FTIR spectra carried out at r.t.
[c] Result of the DSC measurements during the second heating run carried out at 10 °C min^{-1}.

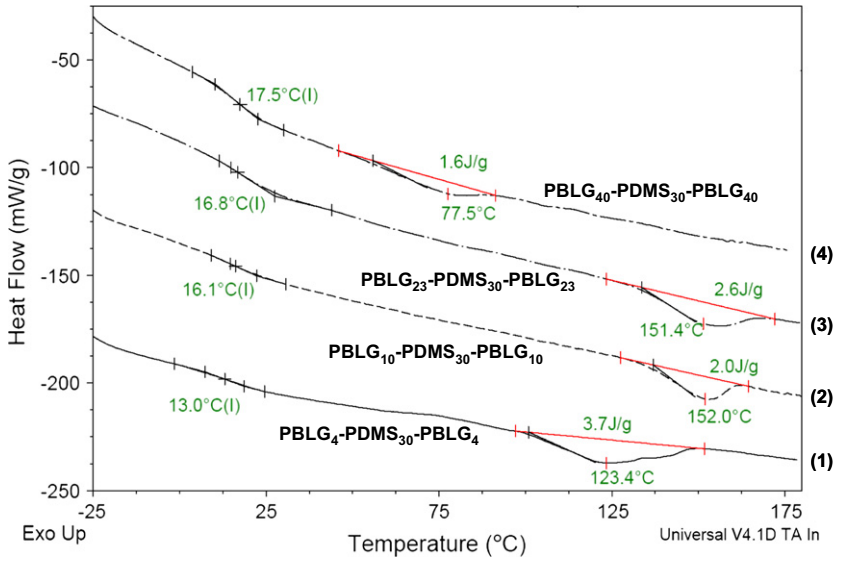

Fig. 2. Differential scanning calorimetry (DSC) thermograms of the triblock copolymers (**1**)–(**4**) obtained during the second heating run (10 °C min^{-1}).

due to the PBLG block. This transition depends on the chain length of the polypeptide and varies between 13 °C for shorter chains and 17 °C for the longer ones. In addition, a further first-order transition was observed. This transition, demonstrated to be reversible during the successive heating and cooling runs, strongly depends on the diblock composition. Whereas for the shortest polypeptide triblock (**1**) the transition occurs at 123 °C, an increase in size has associated with a raise in the transition temperature up to 152 °C for (**2**) and (**3**). On the other hand, an unexpected decrease in the transition temperature has been detected for (**4**) founded at ~77 °C. Since variations not only in the molecular nature but also in the molar comonomers ratio can exert effective control over both the transition temperature and the phase structure [22] we further investigated the nano-structures formed in melt at different temperatures for each block copolymer. For that purpose, we first used small-angle light scattering (SALS) and polarized optical microscopy (POM).

SALS and POM experiments on the block copolymers' series have been carried out at different temperatures, below and above the reversible transition observed in DSC. Whereas (**1**) and (**2**) did not show any pattern in SALS or birefringence in POM at room temperature, (**3**) and (**4**) exhibit in SALS a characteristic four leaf clover (Fig. 3). To the best of our knowledge such a pattern has been found in lamellar structures or in mesostructures formed by the association of cylindrical rods [25]. The POM images of these two last polymers recorded at room temperature show birefringence and also suggest the presence of ordered structures. The SALS patterns of both (**3**) and (**4**) block copolymers disappeared by heating the sample at temperatures above 150 °C and 80 °C, respectively, indicating the transition to a less ordered state. Upon cooling to room temperature the four leaf clover pattern reappeared. Equally, a partial loss of the mesostructure can be observed in the POM images where nevertheless a certain degree of birefringence can still be observed. On the basis of these two experiments we can thus conclude that those systems with higher polypeptide content have a larger tendency to organize (birefringence in the POM images). Depending on the polypeptide fraction, the block copolymer organizes differently at the very large scales (few hundreds of nm): whereas for low polypeptide content (**1**) and (**2**) block copolymers form rather disordered structures, (**3**) and (**4**) produced large-scale superstructures.

As described above, temperature induces important structural changes disturbing the long-range order of PBLG–PDMS–PBLG block copolymers. In order to obtain detailed indeed on the consequences of the thermal treatment on the structure for all the systems we attempted to identify the mesophases developed in these block copolymers by means of small- and wide-angle X-ray scattering (SAXS, WAXS) and Atomic force microscopy (AFM).

At low sample-to-detector distances (WAXS) information both on the local organization of the polypeptide chains and the peptide secondary structures was achieved (Fig. 4). In agreement with the IR spectroscopy results [15], at room temperature, longer polypeptide chains above 20 units, formed stable α-helical secondary structures [26] as observed in the spectra by the presence of reflection peaks at $q \sim 4.5$; 7.9; and 9.0 nm^{-1} characteristic of a two-dimensional hexagonal organization of the polypeptide α-helical rods [27]. Copolypeptides (**1**) and (**2**) show a mixed structure with both α-helical formation and an important contribution of β-sheet as observed by the characteristic reflection peak at $q \sim 3.6$ nm^{-1} (red triangles). WAXS experiments carried out at higher temperatures above the reversible transition (160 °C) (not depicted here), are similar to those carried out at room temperature. The persistence polypeptide helices in (**3**) and (**4**) within this range of temperatures, also observed by Deming et al. [12] confirmed the stability of the helical backbone conformation and excluded eventual morphological changes in the internal polypeptide structure upon heating. As a consequence, the transitions observed in DSC cannot be associated to eventual changes in the local peptide chain.

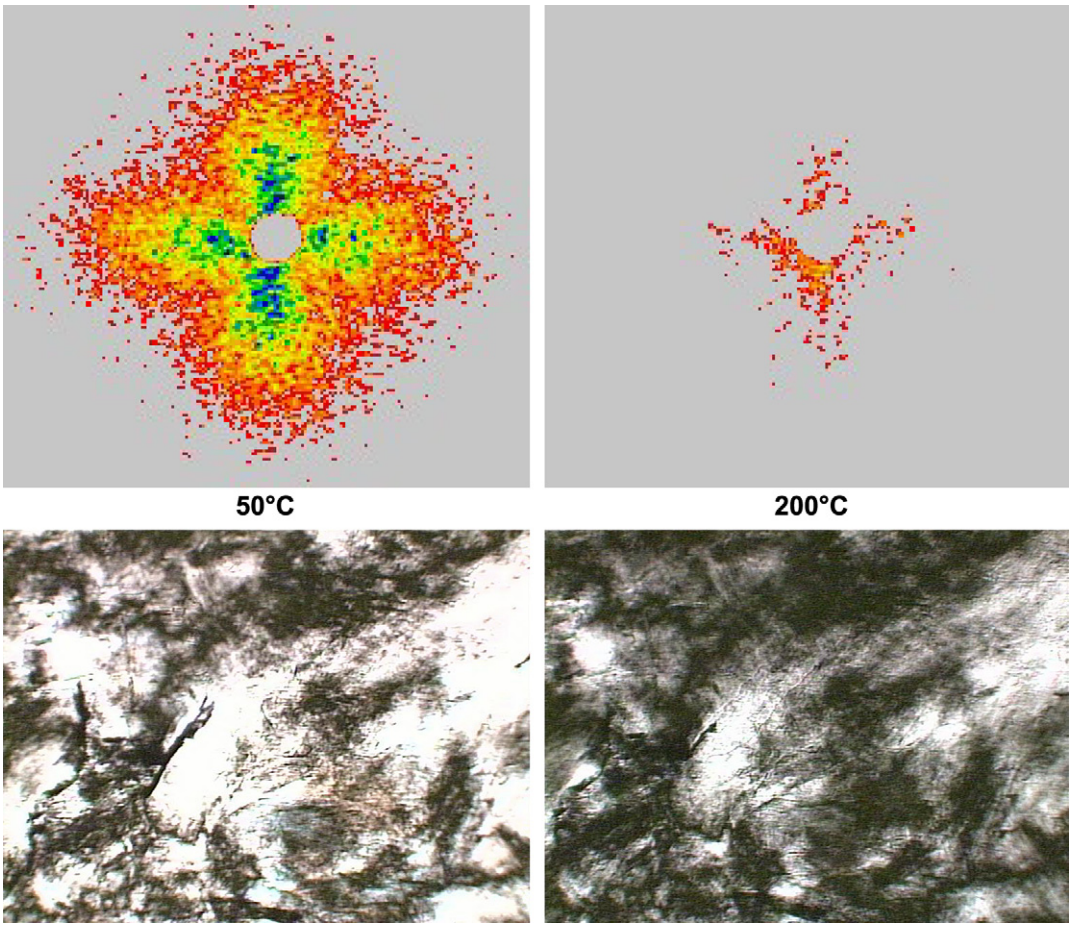

Fig. 3. Representative small-angle light scattering (SALS) (up) and polarized optical microscopy (POM) photographs of block copolymer (**4**) (down) recorded below (at 50 °C) and above (200 °C) the reversible transition.

At longer sample-to-detector distances (SAXS) some important differences are founded between the copolymers. The X-ray spectra of (**1**) and (**2**) show a single and rather large peak at $q \sim 0.92\ \mathrm{nm}^{-1}$ and $q \sim 0.83\ \mathrm{nm}^{-1}$, respectively (Fig. 5b). To the best of our knowledge and since no other reflections can be observed, these patterns could correspond to the formation of randomly oriented imperfect fibers. This hypothesis is in agreement with another several facts: first, with the absence of any signal in SALS and birefringence in POM. Equally, the intense peaks with a *d*-spacing of 7 nm for (**1**) and 8 nm for (**2**) that correspond to the diameter of the fiber, are in good agreement with the calculated length value of the triblock copolymers supposing an extended polypeptide block in its β-sheet conformation (axial translation per residue of 0.35 nm) and a coiled PDMS central block. AFM images of both (**1**) and (**2**) were obtained on films prepared from 1 to 2% THF solutions spin coated on a silicon wafer. Fig. 5(a) depicts the AFM amplitude images obtained using the tapping mode for copolymer (**2**). In spite of the fact that both support and polymer/air interface interactions can, in some cases, dramatically modify the surface morphology this image clearly exhibit the formation of rodlike structures randomly distributed at the surface. Moreover, the thickness of the fiber measured on the AFM images corresponds to the *d*-spacing obtained in SAXS.

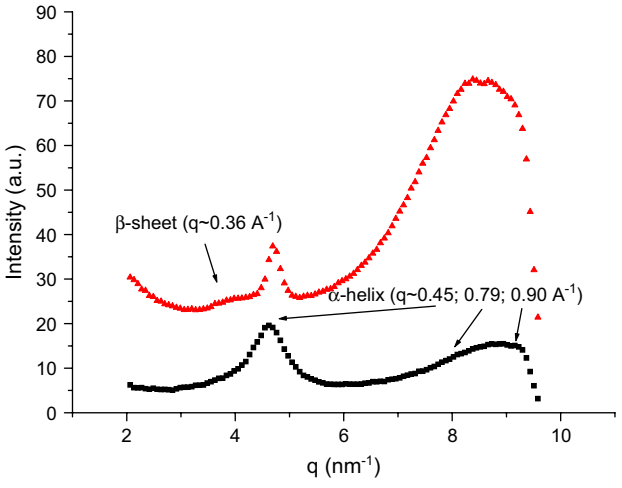

Fig. 4. WAXS patterns of the triblock copolymers at room temperature, (**2**) (triangles) and (**4**) (squares), whereas (**2**) exhibits a local organization composed of a mixed β-sheet polypeptide conformation (reflection at 3.6 nm^{-1}) and α-helical conformation and (**4**) shows exclusively a α-helical secondary structure. The α-helical structure leads to hexagonal packing with peaks at relative positions (1:$\sqrt{3}$:$\sqrt{4}$).

On the basis of the SAXS measurements, the morphologies of polymers (**3**) and (**4**) are significantly different to the previous ones. The SAXS pattern of block copolymer (**3**), at room

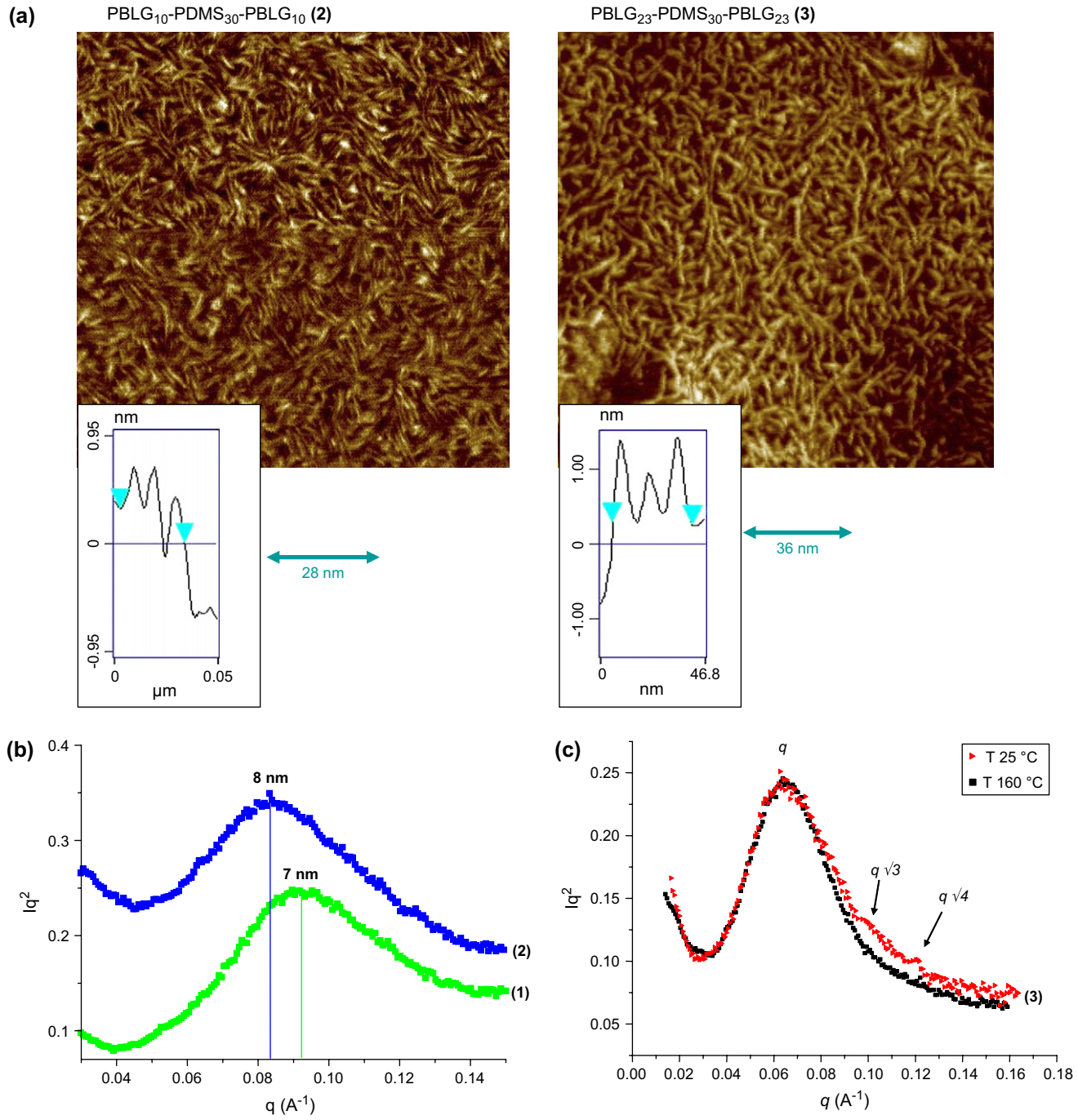

Fig. 5. (a) Phase AFM images of (**2**) left and (**3**) right cast in tetrahydrofuran (1 µm × 1 µm) and sectional view of the fibers formed by (**2**) with a 9 nm thickness and (**3**) with a 12 nm thickness; (b) X-ray patterns of the triblock copolymers $PBLG_4$–$PDMS_{30}$–$PBLG_4$ (**1**) and $PBLG_{10}$–$PDMS_{30}$–$PBLG_{10}$ (**2**); (c) X-ray patterns of the triblock copolymer $PBLG_{23}$–$PDMS_{30}$–$PBLG_{23}$ (**3**) recorded at two different temperatures: 25 °C (red dots) and 160 °C (black dots) sample-to-detector distances of 106 cm. (For interpretation of the references to colours in figure legends and text, the reader is referred to the web version of this article.)

temperature, showed three peaks with a characteristic Bragg spacing in the ratio $1:\sqrt{3}:\sqrt{4}$ (Fig. 5c). Such pattern corresponds to the presence of hexagonally packed cylinders and the overall structure has been previously described as cylinders-on-hexagonal [28]. The major peak at $q \sim 0.6\ nm^{-1}$ corresponds to the distance between the center of two rods and therefore also to the diameter of a single cylinder. It appears that the *d*-spacing of 10 nm can be compared with corresponding distances calculated for perfect α-helices (axial translation per residue of 0.15 nm) with an additional PDMS central block in a random coil conformation. When heated above 160 °C, the mesophase formed seemed to become less ordered since the two reflections related to the hexagonal structure disappeared. Interestingly, this effect is reversible and the hexagonal array can be found again by cooling. On the basis of SAXS and WAXS and according to SALS and

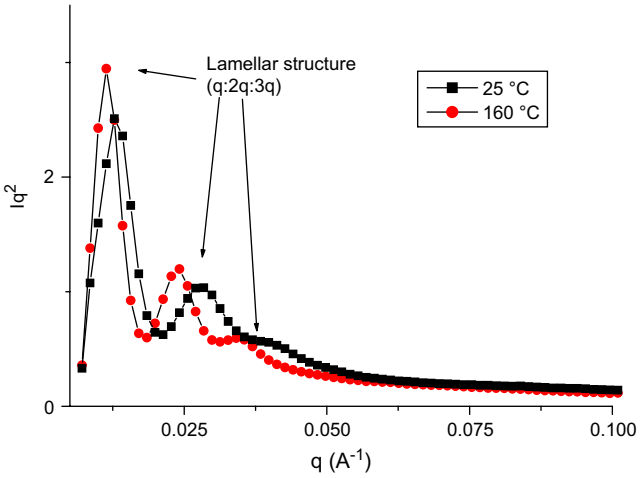

Fig. 6. X-ray patterns of the triblock copolymer (**4**) recorded at two different temperatures: 25 °C (squares) and 160 °C (circles) sample-to-detector distances of 106 cm.

POM, it can be concluded that whereas the rods conserved their internal structure (associated polypeptide chains in its α-helical conformation), the higher-scale hexagonal structure is disrupted during heating.

AFM images obtained for copolymer (**3**) shows the presence of rod structures with diameters of ~12 nm (10 nm in SAXS experiments). Due to the orientation of the fibers parallel to the interface, the detection of the hexagonal packing determined in bulk by using scattering techniques could not be evidenced. We can thus conclude that block copolymers (**1**)–(**3**) lead to the formation of cylinders with thicknesses that increase with the polypeptide chain length and when in bulk, in block copolymer (**3**) the rods are able to associate to form a hexagonal structure (Fig. 6).

The SAXS spectra obtained for (**4**) show three reflection peaks at relative positions 1:2:3 that correspond to a lamellar structure. This structure, also called cylinder-in-lamellar morphology [28], reflects the association of hexagonal helices in cylinders that are embedded in a lamellar phase, and has been also identified by Floudas et al. [29] for the same type of triblock copolymers. Moreover, this structure has been evidenced by AFM imaging (Fig. 7) in thin films with a 25 nm thickness. Under these conditions, the formation of lamellar structures perpendicular to the substrate with a period of 56 nm can be observed. This periodicity is in good agreement with the *d*-spacing result of the SAXS spectra i.e. 50 nm.

The thermal behavior of (**4**) is somehow different from the previous block copolymers. First of all, the transition takes place at lower temperatures, around 80 °C. This effect can be, at least partially, explained by two main causes: the variation of the molar ratio of the comonomers that can exert control both on the transition temperature and the fact that different types of structures could lead to differences in the thermal transitions [30–32]. In spite of the fact that the reflection peaks of the lamellar structure still present at temperatures above the reversible transition a shift on the peaks to lower *q* (higher *d*-spacing) is observed. Although this indicates that the main mesophase structure formed could be kept upon heating, it seems that the lamellar spacing increases at higher temperatures. The structural changes at the local range appeared to have important consequences at the higher-scale order as observed in SALS.

As a consequence of all the results described above we can propose a schematic molecular model that summarizes the structure of the different block copolymers and their thermal behavior (Fig. 8). We attested the presence of three different types of structures depending on the molar fraction peptide/block copolymer. At low peptide contents, for system (**1**) and (**2**) we observed the apparent formation of rather imperfect fibers. Increasing the polypeptide length has a consequence on the stabilization of the α-helical secondary structure that induces order to the system, so that for (**3**)

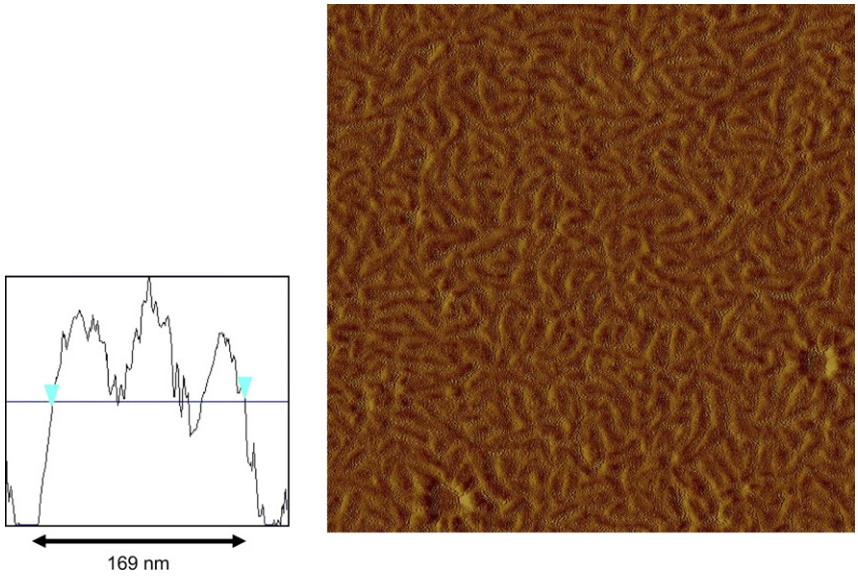

Fig. 7. Phase AFM phase images of (**4**) cast in tetrahydrofuran (2 μm × 2 μm). Left: sectional view of the lamellar phase with a *d*-spacing of 56 nm.

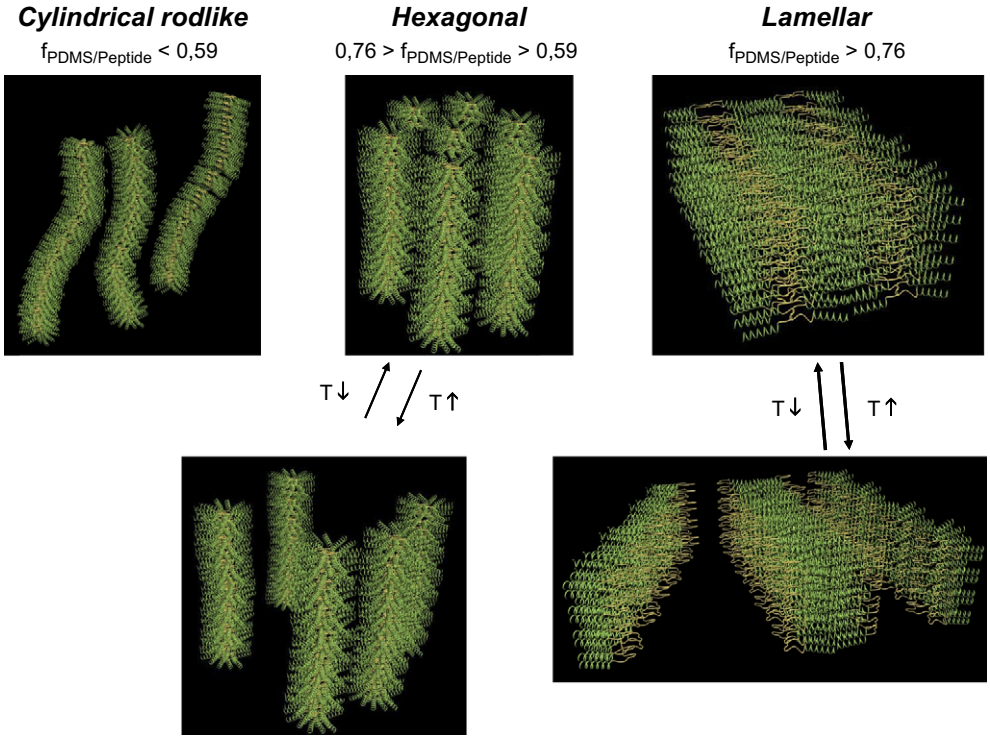

Fig. 8. Model of local organization and thermal transformation proposed for all the triblock copolymers PBLG–PDMS–PBLG.

a cylinder-in-hexagonal and for (**4**) a cylinder-in-lamellar morphology have been found.

All the block copolymers have associated a reversible thermal transition as observed by DSC experiments. Moreover, for systems (**3**) and (**4**) we have been able to associate the thermal transition with significant morphological changes on the higher-scale self-assembled structure. As a result, we demonstrate that when copolymer (**3**) is heated above 160 °C the hexagonal packing is disrupted and has consequences to a longer range of order (as detected by POM and SALS). Upon heating block copolymer (**4**) up to 80 °C, the global lamellar structure formed at room temperature is retained but the spacing between the single lamella is increased and perturbed the formation of higher scale structures. The supramolecular order observed by SALS and POM in (**3**) and (**4**) is recovered by cooling at r.t. and evidenced the reversibility of the thermal transition.

In this contribution we described the thermal behavior and the nano-organization of rod–coil–rod triblock copolymers PBLG–PDMS–PBLG. These block copolymers have been designed to contain a rigid rod liquid crystal PBLG and a soft central block having the role of inducing thermotropical behavior in the material. The different structures formed in bulk have been identified using SALS, POM and X-ray scattering (SAXS and WAXS) experiments. Short polypeptide chains up to 23 units favored the formation of fibrillar structures. The fibers formed in block copolymer (**3**) lead by their association to a hexagonal structure. Triblock copolymers formed by longer polypeptide chains preferred to join together in a lamellar structure. The thermotropic behavior has been evidenced by DSC experiments. All the block copolymers exhibit in DSC thermograms a reversible transition that has been identified in terms of structural changes.

Acknowledgments

Financial support from CNRS and region Aquitaine is gratefully acknowledged.

References

[1] Hadjichristidis N, Pispas S, Floudas G. Block copolymers: synthetic strategies, physical properties and applications. Wiley-Interscience; 2002.
[2] Gil ES, Hudson SM. Prog Polym Sci 2004;29:1173.
[3] Iwata H, Oodate M, Uyama Y, Amemiya H, Ikada Y. J Membr Sci 1991; 55:119.
[4] Crevoisier GD, Fabre P, Corpart JM, Leibler L. Science 1999;285:1246.
[5] Huber DL, Manginell RP, Samara MA, Kim B, Bunker BC. Science 2003;301:352.
[6] Demus D, Goodby J, Gray GW, Spiess HW, Vill V. Handbook of liquid crystals. New York: Wiley-VCH; 1998.
[7] Percec V, Tsuda Y. Side chain liquid crystal polymers. New York: Chapman and Hall; 1989.
[8] Percec V, Tsuda Y. Macromolecules 1990;23:5.
[9] Watanabe J, Ono H, Uematsu I, Abe A. Macromolecules 1985;18:2141.
[10] Watanabe J, Tominaga T. Macromolecules 1993;26:4032.
[11] Guillermain C, Gallot B. Macromol Chem Phys 2002;203:1346.
[12] Schaefer KE, Keller P, Deming TJ. Macromolecules 2006;39:19.
[13] Watanabe J, Fukuda Y, Gehani R, Uematsu I. Macromolecules 1984;17: 1004.
[14] Watanabe J, Goto M, Nagase T. Macromolecules 1987;20:298.
[15] Ibarboure E, Rodriguez-Hernandez J, Papon E. J Polym Sci Part A Polym Chem 2006;44:4668.
[16] Nakajima A, Hayashi T, Kugo K, Shinoda K. Macromolecules 1979;12: 840.
[17] Nakajima A, Kugo K, Hayashi T. Macromolecules 1979;12:844.

[18] Floudas G, Papadopoulos P, Klok H-A, Vandermeulen GVM, Rodriguez-Hernandez J. Macromolecules 2003;36:3673.
[19] Daly WH, Poche D. Tetrahedron Lett 1988;29:5859.
[20] Kumaki T, Sisido M, Imanishi Y. J Biomed Mater Res 1985;19:785.
[21] Deming TJ. J Polym Sci Part A Polym Chem 2000;38:3011.
[22] Klok H-A, Lecommandoux S. Adv Mater 2001;13:1217.
[23] Klok H-A, Langenwalter JF, Lecommandoux S. Macromolecules 2000; 33:7819.
[24] Kuo ACM. Polymer data handbook. New York: Oxford University Press; 1999.
[25] Borch J, Muggli R, Sarko A, Marchessault RH. J Appl Phys 1971;42: 4570.
[26] Papadopoulos P, Floudas G, Klok H-A, Schnell I, Pakula T. Biomacromolecules 2004;5:81.
[27] Minich EA, Nowak AP, Deming TJ, Pochan DJ. Polymer 2004;45:1951.
[28] Papadopoulos P, Floudas G, Schnell I, Aliferis T, Iatrou H, Hadjichristidis N. Biomacromolecules 2005;6:2352.
[29] Papadopoulos P, Floudas G, Schnell I, Lieberwirth I, Nguyen TQ, Klok H-A. Biomacromolecules 2006;7:618.
[30] Laus M, Bignozzi MC, Angeloni AS, Galli G, Chiellini E. Macromolecules 1993;26:3999.
[31] Craig AA, Imrie CT. Polymer 1997;38:4951.
[32] Tang H, Zhu Z, Wan X, Chen W, Zhou Q. Macromolecules 2006;39: 6887.